

Thermodynamics of Hydrogen Bonding in Hydrophilic and Hydrophobic Media

David van der Spoel,^{*,†} Paul J. van Maaren,[†] Per Larsson,[‡] and Nicușor Tîmneanu[†]

Department of Cell and Molecular Biology, Uppsala University, Husargatan 3, Box 596, SE-751 24 Uppsala, Sweden, and Stockholm Bioinformatics Center, Stockholm University, SE-10691 Stockholm, Sweden

Received: December 12, 2005

The thermodynamics of hydrogen bond breaking and formation was studied in solutions of alcohol (methanol, ethanol, 1-propanol) molecules. An extensive series of over 400 molecular dynamics simulations with an aggregate length of over 900 ns was analyzed using an analysis technique in which hydrogen bond (HB) breaking is interpreted as an Eyring process, for which the Gibbs energy of activation ΔG^\ddagger can be determined from the HB lifetime. By performing simulations at different temperatures, we were able to determine the enthalpy of activation ΔH^\ddagger and the entropy of activation $T\Delta S^\ddagger$ for this process from the Van't Hoff relation. The equilibrium thermodynamics was determined separately, based on the number of donor hydrogens that are involved in hydrogen bonds. Results (ΔH) are compared to experimental data from Raman spectroscopy and found to be in good agreement for pure water and methanol. The ΔG as well as the ΔG^\ddagger are smooth functions of the composition of the mixtures. The main result of the calculations is that ΔG is essentially independent of the environment (around 5 kJ/mol), suggesting that buried hydrogen bonds (e.g., in proteins) do not contribute significantly to protein stability. Enthalpically HB formation is a downhill process in all substances; however, for the alcohols there is an entropic barrier of 6–7 kJ/mol, at 298.15 K, which cannot be detected in pure water.

1. Introduction

Water is the single most important prerequisite for life as we know it.¹ Its small size and ability to form and break hydrogen bonds (HBs) on the picosecond time scale, allow it to act as a lubricant for conformational transitions in biomolecules,^{2,3} or even to function as catalyst for the folding of proteins.⁴ In the context of protein folding, partitioning of hydrophobic and hydrophilic groups is of crucial importance. A simple model system that contains both such groups is made up by solutions of short alcohol molecules. Obviously, the solubility of alcohols in water decreases with increasing chain length, due to aggregation of aliphatic groups. A recent neutron diffraction study of a methanol/water mixture⁵ has provided direct structural proof for the hypothesis that molecular segregation occurs even for the shortest alcohol in aqueous solution. This notion is further supported by recent neutron-scattering experiments and simulations which seem to indicate that in a mixture of water and methanol both components form a percolating network.⁶ We have recently shown that classical molecular dynamics (MD) simulations can be used to simulate the properties of alcohol/water mixtures.⁷ Moreover, we have demonstrated that thermodynamic (energy and density) and dynamic properties (diffusion and viscosity) can be reproduced for aqueous solutions of methanol (MeOH), ethanol (EtOH), and 1-propanol (PrOH).⁷ In this paper we report on the simulated HB thermodynamics in alcohol/water mixtures spanning the whole composition range from 0 to 100% alcohol in steps of 10 mass %. We derive the thermodynamic parameters that govern HB breaking and compute the equilibrium thermodynamics from simulations at different temperature. Together this

allows us to completely describe the energetics of the process of HB breaking in these substances and to draw conclusions about the effect of the environment on the HB breaking kinetics and equilibria.

2. Methods

In total 31 systems were simulated, starting from 1000 water molecules, in steps of 100 water molecules down to 0, with compensating amounts of either MeOH, EtOH, or PrOH, such as to make up a mass fraction of 0%, 10%, etc. up to 100 alcohol. All simulations were performed three times with different starting conformations at 288.15, 298.15, and 308.15 K, to improve statistics. The OPLS force field⁸ was used for the alcohol molecules, and it was combined with the TIP4P water model.⁹ The smooth particle-mesh Ewald (PME) algorithm¹⁰ was used for long-range electrostatics interactions, since any method that does not take long-range electrostatics into account faces severe artifacts.^{11,12} The GROMACS 3.2.1 software was used for all simulations;^{13,14} HB analysis was performed using GROMACS 3.3.¹⁵ Further simulation details are given in ref 7. Equilibration of the simulations was checked by monitoring the potential energy and density. In all cases these values had equilibrated within 50 ps. To be on the safe side, the first 200 ps of the simulations were discarded, leaving 2 ns for analysis. The coordinates were saved every 200 fs in the production simulations. However, for a more thorough analysis of the effect of the saving frequency on the HB lifetimes, shorter simulations of 500 ps were done for pure water, MeOH, EtOH, and PrOH, in which the coordinates were saved every 10, 20, 50, and 100 fs, respectively.

Four further sets of simulations were performed using different water models: TIP3P,⁹ TIP5P,¹⁶ SPC,¹⁷ and SPC/E.¹⁸ These simulations were performed once at each of the three temperatures mentioned above under otherwise identical conditions.

* To whom correspondence may be addressed: tel, 46-18-4714205; fax, 46-18-511755; e-mail, spoel@xray.bmc.uu.se.

[†] Uppsala University.

[‡] Stockholm University.

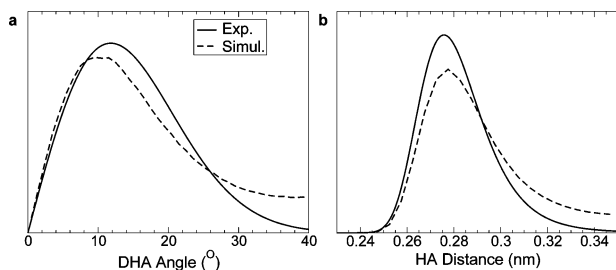


Figure 1. (a) HB angle distribution in water from NMR experiments²¹ and from simulation using the TIP4P⁹ model. (b) Donor-acceptor distance. In the experimental source²¹ the hydrogen-acceptor distance was determined. The whole figure was shifted by 0.089 nm such that the peak lies at 0.275 nm, corresponding to the peak in the experimental radial distribution function.²³

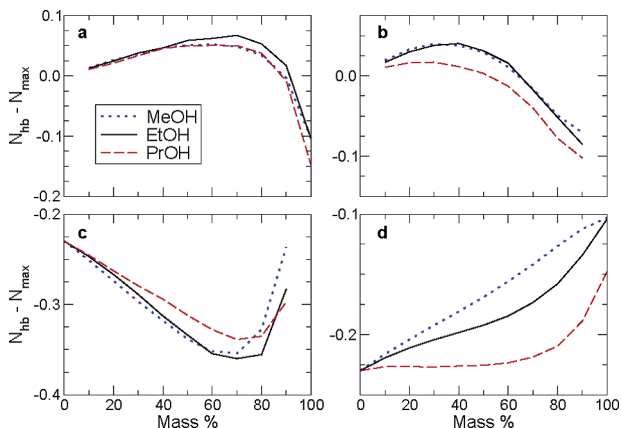


Figure 2. Number of HBs, N_{hb} , minus the theoretical maximum, N_{max} , per molecule in four categories: (a) alcohol-alcohol; (b) alcohol-water; (c) water-water; (d) total. There is a surplus in alc-alc and alc-wat HBs, up until a 70–80 mass %.

3. Results

3.1. Number of Hydrogen Bonds. HBs can be defined in different ways, either based on geometry—donor—hydrogen—acceptor (DHA) angle and donor—acceptor (DA) or hydrogen—acceptor (HA) distance—or based on interaction energy and distance (although the differences are minor¹⁹). For comparison with earlier studies we employed a geometrical criterion with a maximum DA distance of 0.35 nm and a DHA angle of 30°. With this definition we reproduce exactly the average number of HBs per molecule in pure TIP4P water (1.77) of Xu and Berne.²⁰ The distribution of HB geometries in water was determined experimentally recently²¹ using an innovative nuclear magnetic resonance technique.²² If we compare the experimental HB geometry with the simulated one (Figure 1), we see that the DHA angle distributions are similar but the experimental one falls off more rapidly. The DA distance distribution also shows these features, indicating that the simulation, which employs effective pair potentials, slightly underestimates the strength and localization of the HB.

The numbers of HBs per molecule, minus the theoretical maximum number of HBs (N_{max} , see Appendix A), are shown in Figure 2 as a function of alcohol mass fraction. The total number of HBs for MeOH/water (Figure 2d) is a straight line, indicating that as far as hydrogen bonding is concerned this is a perfect mixture. For EtOH and PrOH solutions there is a minimum with respect to a straight line indicating that there are fewer HBs than the theoretical maximum. Both the number of alc-alc and alc-wat HBs are found to be higher than those expected theoretically (parts a and b of Figure 2). In contrast the number of wat-wat HBs is substantially less than expected

TABLE 1: Uninterrupted Hydrogen Bond Lifetimes τ_1 at $T = 298.15$ K Calculated from Equation 1 from Coordinates Saved at Interval Δt^a

simulation	τ_1 (ps)					
	$\Delta t = 0$	$\Delta t = 10$ fs	$\Delta t = 20$ fs	$\Delta t = 50$ fs	$\Delta t = 100$ fs	$\Delta t = 200$ fs
water	0.15	0.22	0.27	0.46	0.77	1.15
MeOH	0.17	0.33	0.48	0.89	1.44	2.11
EtOH	0.17	0.40	0.59	1.13	1.90	2.71
PrOH	0.21	0.35	0.50	0.98	1.69	2.45

^a To obtain a value of $\Delta t = 0$, cubic spline interpolations through the five other points were made, which were subsequently extrapolated to $\Delta t = 0$. The errors in these values are less than 1%.

(Figure 2c) which leads to the conclusion that the HB network in water is seriously disrupted upon the addition of alcohol molecules, even though the alcohol molecules are forced together (Figure 2a).

3.2. Hydrogen Bond Lifetimes. HB lifetimes can be computed in different ways, depending not only on the definition of the HB that is used (see above) but also on the choice of what to regard as a continuous HB. Should a HB that is broken according to the definition when it re-forms (somewhat) later be regarded as the same HB or as a new HB? Both definitions are tested and discussed below.

3.2.1. Continuous Hydrogen Bonds. If one decides that a HB must exist continuously (the uninterrupted HB²⁴), one can compute a distribution of lifetimes $P(t)$ by making a histogram of the number of HBs that existed continuously from time 0 to t . The probability of breaking a hydrogen bond is constant and independent of the history of the bond, and hence the tail of the $P(t)$ curve should fall off exponentially;^{19,25} this is indeed what we find. The lifetime distribution can be converted into an autocorrelation function by

$$C(t) = 1 - \int_0^t P(\tau) d\tau \quad (1)$$

An overall HB lifetime τ_1 can now be associated with the integral of eq 1

$$\tau_1 = \int_0^\infty C(t) dt \quad (2)$$

Results for the different systems and different frequency of saving Δt coordinates are given in Table 1.

In molecular dynamics simulations one uses a finite time step and saves coordinates every Δt (ps), where Δt is as small as one can afford in terms of disk space usage (for the simulations presented in this paper more than 300 GB of data were generated). Obviously $P(t)$, and hence τ_1 , depends heavily on the saving interval. The reason for this is that if we sample more often, any breaking event for a HB will shift the $P(t)$ curve to the left. To get an estimate for the “real” HB lifetime, we have extrapolated the lifetimes to $\Delta t = 0$ (using a cubic spline interpolation, Table 1). However, we cannot deduce the zero-interval results for simulations in which we have saved coordinates at 200 fs only (more than 400 production simulations); for instance, EtOH has a smaller “real” τ_1 than PrOH, whereas for the simulation where we stored coordinates with interval $\Delta t = 200$ fs only, the order is reversed. Starr et al.¹⁹ used the uninterrupted HB definition (the “history-dependent” HB in their terminology) for an analysis of supercooled water and sampled the simulation every 10 fs. According to our cubic spline interpolation the HB lifetime in TIP4P water at a 10 fs sampling interval is 0.22 ps, compared to 0.15 ps at 0 fs

sampling interval (Starr et al.¹⁹ find 0.27 ps for SPC/E water¹⁸ which has stronger HBs due to larger partial charges). Thus, even by sampling 20 times as often as we did in this work (increasing our combined trajectory size to over 2 TB), we would still not have a good enough approximation of the lifetimes. The uninterrupted HB definition for analysis of HB lifetime distributions therefore should therefore be regarded as impractical.

3.2.2. Interrupted Hydrogen Bonds. If we allow HBs to break and re-form, we can analyze HB lifetimes by defining a binary function $h(t)$, which is 1 when a H bond is present and 0 otherwise.²⁵ The autocorrelation function $c_h(t)$ of $h(t)$ was computed and averaged over similar types of HBs. In the terminology of Luzar,²⁴ this is the “intermittent HB correlation function”, which by design is insensitive to the saving frequency Δt , except for the very shortest times ($0 \leq t \leq \Delta t$). Since the simulation systems are finite, the $c_h(t)$ do not go to zero and the $c_h(t)$ have to be scaled to zero at long times.¹⁹ In the remainder of this paper we will use this definition for the analysis of kinetics and thermodynamics of hydrogen bonding.

3.3. Kinetics of Hydrogen Bonding. The kinetics of hydrogen bond breakage and re-formation can be derived from a chemical dynamics analysis.^{25,24} Here, a forward rate constant k for HB breakage and a backward rate constant k' for HB formation are determined from the reactive flux correlation function $K(t)$

$$K(t) = -\frac{dc_h(t)}{dt} \quad (3)$$

and

$$K(t) = kc_h(t) - k'n(t) \quad (4)$$

where $n(t)$ is the probability that a HB is broken that existed at $t = 0$ but that the two hydrogen bonding groups are still within hydrogen bonding distance. The hydrogen bond lifetime in this scheme is given by the inverse forward rate constant

$$\tau_{\text{HB}} = 1/k \quad (5)$$

In the Supporting Information (Tables 1–3) k and k' are given as a function of concentration and for three different temperatures. The rates decrease monotonically with alcohol concentration; the forward (breaking) rates are 1.7 (MeOH) to 2.2 (EtOH, PrOH) times lower in the pure alcohols than in water. As expected, the rates increase with increasing temperature in all cases.

3.4. Thermodynamics of Hydrogen Bond Breaking. If we assume that the process of HB breakage can be described as an Eyring process, we can relate τ_{HB} (eq 2) to the Gibbs energy of activation ΔG^\ddagger

$$\tau_{\text{HB}} = \frac{h}{k_B T} \exp\left(\frac{\Delta G^\ddagger}{k_B T}\right) \quad (6)$$

where h is Planck's constant, k_B is Boltzmann's constant, and T is the temperature. We can then derive the activation enthalpy of HB breaking ΔH^\ddagger from the Van't Hoff equation

$$\Delta H^\ddagger = \frac{\partial(\Delta G^\ddagger/T)}{\partial(1/T)} \quad (7)$$

and hence the entropy of activation $T\Delta S^\ddagger = \Delta H^\ddagger - \Delta G^\ddagger$. The thermodynamical parameters are plotted in Figure 3 (data in

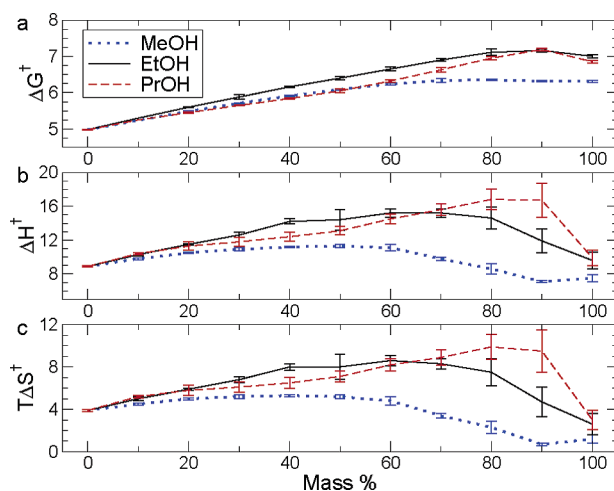


Figure 3. Activation thermodynamics (kJ/mol) as a function of alcohol concentration. Error bars in ΔG^\ddagger are derived from the errors in rate constants determined from three simulations. The error bars in ΔH^\ddagger follow from the temperature derivative of the errors in ΔG^\ddagger ; errors in $T\Delta S^\ddagger$ are assumed to be identical to those in the corresponding ΔH^\ddagger .

the Supporting Information, Table 4). For all three alcohols the ΔG^\ddagger are smooth functions of the concentration with a very slight maximum between 80 and 90%. There are maxima for ΔH^\ddagger at 50% for MeOH, at 60% for EtOH, and at 80% for PrOH (but with considerable error bars). Although the ΔH^\ddagger are quite high, especially at intermediate to high alcohol concentrations, this is to a large extent compensated for by the considerable entropy ($T\Delta S^\ddagger$) increase upon HB breaking.

From the number of HBs (N_{hb} , Figure 2) we can in principle derive an equilibrium constant

$$k_{\text{eq}} = \frac{N_{\text{hb}}}{N_{\text{max}} - N_{\text{hb}}} \quad (8)$$

where N_{max} is the maximum number of HBs (Appendix A). However, to be able to compare our results directly to experimental data from Raman spectroscopy,^{26–29} we have to determine another parameter, namely, the number of donor hydrogens that are free (not hydrogen bonded), and determine an equilibrium constant from that

$$k_{\text{eq}} = \frac{N_{\text{max}} - N_{\text{free}}}{N_{\text{free}}} \quad (9)$$

The difference between the two quantities arises from the fact that according to our HB criterion one H may be involved in two hydrogen bonds, and hence eq 8 will slightly overestimate k_{eq} . Using k_{eq} from eq 9 we can determine the free energy of hydrogen bonding

$$\Delta G = k_B T \ln k_{\text{eq}} \quad (10)$$

The enthalpy ΔH and entropy $T\Delta S$ are again determined from the Van't Hoff equation (cf. eq 7). All results are presented in the Supporting Information, Table 5.

ΔG is a smooth function of the alcohol concentration for all types of HBs (Figure 4a). For MeOH and EtOH solutions, ΔG is nearly constant with alcohol concentration indicating that the fraction of all the possible HBs that is actually formed is independent of the environment. In PrOH/water ΔG does fall off somewhat at high alcohol concentration, probably because it is more difficult to maintain a high fraction of all the possible HBs. ΔH (Figure 4b) can be directly compared to Raman

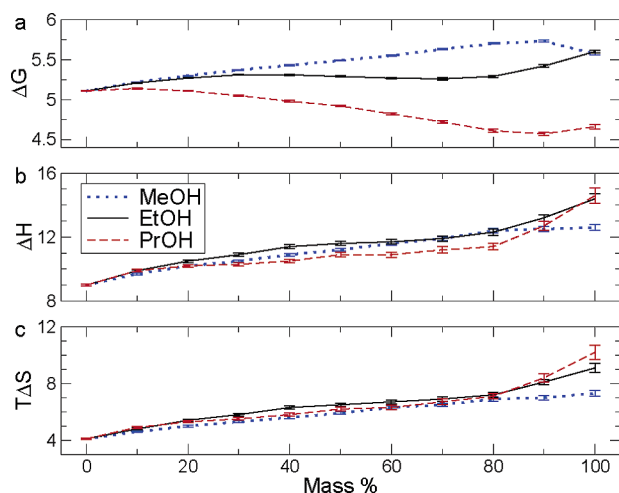


Figure 4. Equilibrium thermodynamics (kJ/mol) as a function of alcohol concentration. Error bars are computed in the same fashion as those in Figure 3.

TABLE 2: Equilibrium Enthalpy (kJ/mol) of Hydrogen Bonding for Pure Substances at $T = 298.15$ K^a

	ΔH		
	sim	Raman	NMR
water	9.0(0.05)	10.6(0.5) [ref 26]	
MeOH	12.6(0.2)	11.3(0.1) [ref 29]	12.8 [ref 39]
EtOH	14.4(0.3)	10.5(0.1) [ref 28]	16.8 [ref 39]
PrOH	14.6(0.5)	≈ 11 [ref 30]	

^a Errors within parentheses, determined from a block averaging procedure.³⁸ References to the experimental data for ΔH are given.

spectroscopy experiments that track the amount of hydrogen atoms that are hydrogen bonded.^{26,27} Table 2 presents a comprehensive overview of simulated and experimental results for the pure liquids. Carey and Korenowski find ΔH for pure water to be 10.6 ± 0.5 kJ/mol (this work, 9.0 ± 0.05 kJ/mol). For pure MeOH, Edwards and Farwell²⁹ found 11.3 ± 0.1 kJ/mol (this work, 12.6 ± 0.1 kJ/mol). The simulation results correspond very well with the experimental data for these substances. For EtOH, Edwards et al. found a comparable number of 10.5 kJ/mol²⁸ (this work, 14.4 ± 0.3) while for PrOH only an estimate of 11 kJ/mol is found³⁰ (this work, 14.6 ± 0.5). Obviously the correspondence for the larger alcohols is not as good as that for MeOH and water. Sun et al. found very similar values for ΔH (14.7–16.4 kJ/mol) of PrOH in different media when they tried to model retention of alcohol molecules in gas–liquid chromatography.³¹ It has been shown³² that the description of hydrophobic hydration in EtOH solutions can be improved considerably by using polarizable models, and this is probably the road to greater accuracy in molecular simulation.^{32–35} For instance, Figure 1 shows that the localization of the HB is not described sufficiently well using an empirical nonpolarizable potential such as TIP4P. Finally, nuclear magnetic resonance experiments have also been employed in order to determine the number of HBs in solution,³⁶ and from these, an estimate of ΔH was presented. The enthalpies found in this manner are incompatible with those found using Raman spectroscopy as has been discussed extensively by Lalanne et al.,³⁷ and hence the values determined from Raman spectroscopy should probably be regarded as the reference values.

4. Discussion

For pure water, HB dynamics has been studied by MD simulations in great detail.^{19,20,25,40–43} An important observation

TABLE 3: Activation and Equilibrium Thermodynamics (kJ/mol) of Hydrogen Bonding for Different Water Models at $T = 298.15$ K^a

model	ΔG^\ddagger	ΔH^\ddagger	$T\Delta S^\ddagger$	ΔG	ΔH	$T\Delta S$
TIP3P	3.95	4.5	0.5	3.99	7.0	3.0
TIP4P	4.98	8.9	3.9	5.11	9.0	4.1
TIP5P	4.78	14.8	10.0	3.93	11.1	7.2
SPC	4.67	6.8	2.2	4.55	7.8	3.3
SPC/E	5.70	11.3	5.6	5.36	9.0	3.6

^a The errors in these numbers are comparable to those in Tables 4 and 5 (Supporting Information), i.e., 0.01 kJ/mol for ΔG^\ddagger and ΔG , and 0.1 kJ/mol for the other values.

by Luzar and Chandler was that the HB kinetics is not governed by a single process, since the decay of the HB correlation function is not compatible with a single exponential.²⁵ Instead, they propose a combination of an exponential process and a diffusive decay (drifting apart of two molecules), a mechanism similar in nature to the proposed tetrahedral displacement model for dielectric relaxation.⁴⁴ Using the Luzar and Chandler description of HB kinetics,²⁵ we have determined rate constants for HB breaking and re-forming for alcohol solutions at different temperatures and concentrations. The thermodynamics of activation derived from the HB lifetime (eq 5) shows that there is a considerable enthalpic penalty for HB breaking (Figure 3), particularly in the EtOH and PrOH solutions. The ΔH^\ddagger are compensated for by a considerable increase in $T\Delta S^\ddagger$ leading to a moderate ΔG^\ddagger varying from 6 to 7 kJ/mol.

Schreiner et al. have recently studied HB dynamics in a peptide/water system.⁴⁵ For pure TIP3P⁹ water they find an activation energy E_A of 8–9 kJ/mol based on the rate-constant formalism of Luzar and Chandler,^{25,24} which is quite a bit lower than what we find for TIP4P ($E_A = \Delta H^\ddagger + k_B T = 11.4$ kJ/mol). To verify our calculations, we did the same analysis on a number of water models, including TIP3P (Table 3). For TIP3P we find $E_A = 7$ kJ/mol, which is close to the value of Schreiner et al., and hence we conclude that our calculations are correct. The difference may be explained by the difference in water models, as TIP3P is known to be quite a bit more “slippery” than TIP4P.⁴⁶ For peptide–peptide HBs Schreiner et al. find an E_A which is remarkably similar (8 kJ/mol) to water–water HBs but roughly twice as high as peptide–water HBs. Sheu et al. have reported the activation energies for the rupture of a HB to be 6.6 kJ/mol in a β -sheet and 8.3 kJ/mol in an α -helix.⁴⁷ They argue that these values represent Gibbs energies of activation ΔG^\ddagger rather than ΔH^\ddagger . These numbers are somewhat higher than those that we find for ΔG^\ddagger : 5.1 kJ/mol (water), 5.6 kJ/mol (MeOH), 5.6 kJ/mol (EtOH), and 4.7 kJ/mol (PrOH). Since HB breakage usually takes place by exchange with another HB, the numbers found for peptides are influenced by the water model used in the simulations. Obviously the barrier for breaking HBs is much too low in TIP3P water (cf. Tables 2 and 3), but how this will affect the simulated HB breaking rates in proteins is not clear.

When combining the activation and equilibrium thermodynamics, we can paint the complete picture of hydrogen bonding (Figure 5). The most important finding here is that the equilibrium Gibbs energy ΔG is almost the same for all of the substances, but the ΔG^\ddagger are somewhat larger in nonpolar than in polar environments. In the nonpolar environment there is an enthalpic penalty for moving from the transition state to the unbound state because diffusion of hydrogen bonding groups through hydrophobic media is unfavorable. In watery solutions of alcohols, as in solvated peptides, water can mediate HB reshuffling and “catalyze” the interconversion of peptide

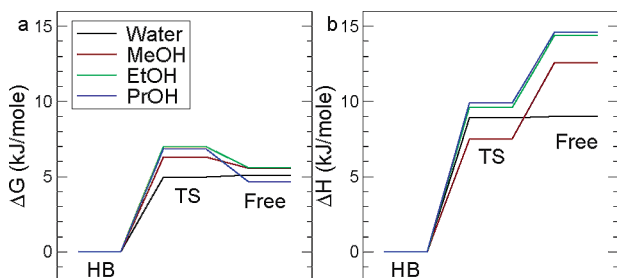


Figure 5. Thermodynamics along the HB breaking pathway in pure fluids: (a) Gibbs energy and (b) enthalpy. Indicated on the *x*-axis are the reactant state (HB), the transition state (TS), and the product state (free).

structures^{2,3} since the typical HB lifetimes are on the order of 2–3 ps (Tables 1–3, Supporting Information). The “lubrication” effect that has been attributed to water⁴ is clearly implicated from our results. Since the stability of HBs (ΔG) does not depend on the environment (Figure 4a), it is probably not correct to assume that HBs contribute significantly to the thermodynamic stability of proteins.⁴⁸ Rather, we find that the enthalpy (ΔH) for HB breaking is larger in water-depleted than in water-rich environments, suggesting that HB exchange is the likely mechanism to breaking HBs.⁴² Therefore it seems likely that the HBs inside a protein yield a large barrier to unfolding, or in other words, they provide kinetic stability rather than thermodynamic stability.

The contribution of hydrogen bonds to protein stability has been studied for a long time. Dill⁴⁹ proposed that protein stability is dominated by the hydrophobic effect. Others like Pace^{50,51} have argued that buried polar groups do contribute significantly to protein stability. Interestingly, Takano et al. find that a Trp side chain that makes a hydrogen bond contributes with 5.4 kJ/mol of stability (ΔG) whereas a buried Trp side chain that does not make a HB contributes 1.7 kJ/mol.⁵¹ The difference between these numbers is 3.7 kJ/mol, very close to the ΔG of 4.7 kJ/mol we find for breaking a HB in PrOH solution. It is not obvious that we can generalize the results presented here on alcohol solutions to protein systems, in particular because proteins are more ordered than solutions or liquids.⁵² The effects we see on HB breaking when moving from a hydrophilic to more hydrophobic environment are probably general.

Acknowledgment. We express our gratitude to Abraham Szöke for useful suggestions. The national supercomputer center in Linköping, Sweden, is acknowledged for allocation of computer time.

Appendix A. Maximum Number of Hydrogen Bonds

Given the number of water molecules N_W and alcohol molecules N_a in a mixture, the theoretical maximum number of hydrogen bonds N_{\max} can be calculated based on the probabilities of making bonds in a perfect mixture. Assuming each alcohol molecule can make one and each water molecule two HBs, we have for alcohol–alcohol bonds

$$N_{\max}(\text{alc} - \text{alc}) = \frac{N_a - 1}{N_a + 2N_W - 1} \quad (11)$$

for water–water bonds

$$N_{\max}(\text{wat} - \text{wat}) = \frac{4N_W - 4}{N_a + 2N_W - 2} \quad (12)$$

for alcohol–water bonds

$$N_{\max}(\text{alc} - \text{wat}) = \frac{2N_a N_W (2N_a + 4N_W - 3)}{(N_a + N_W)(N_a + 2N_W - 1)(N_a + 2N_W - 2)}$$

and for the total number of bonds

$$N_{\max}(\text{total}) = \frac{N_a + 2N_W}{N_a + N_W}$$

Supporting Information Available: Supporting Information comprising tables with rate constants for HB breaking and reforming and for equilibrium and activation thermodynamics. This material is available free of charge via the Internet at <http://pubs.acs.org>.

References and Notes

- (1) Ball, P. *H₂O A biography of water*; Weidenfeld and Nicolson: London, 1999.
- (2) Barron, L. D.; Hecht, L.; Wilson, G. *Biochemistry* **1997**, *36*, 13143–13147.
- (3) Reat, V.; Dunn, R.; Ferrand, M.; Finney, J. L.; Daniel, P. M.; Smith, J. C. *Proc. Natl. Acad. Sci. U.S.A.* **2000**, *97*, 9961–9966.
- (4) Xu, F.; Cross, T. A. *Proc. Natl. Acad. Sci. U.S.A.* **1999**, *96*, 9057–9061.
- (5) Dixit, S.; Crain, J.; Poon, W. C. K.; Finney, J. L.; Soper, A. K. *Nature* **2002**, *416*, 829–832.
- (6) Dougan, L.; Bates, S. P.; Hargreaves, R.; Fox, J. P.; Crain, J.; Finney, J. L.; Réat, V.; Soper, A. K. *J. Chem. Phys.* **2004**, *121*, 6456–6462.
- (7) Wensink, E. J. W.; Hoffmann, A. C.; van Maaren, P. J.; van der Spoel, D. *J. Chem. Phys.* **2003**, *119*, 7308–7317.
- (8) Jorgensen, W. L.; Maxwell, D. S.; Tirado-Rives, J. *J. Am. Chem. Soc.* **1996**, *118*, 11225–11236.
- (9) Jorgensen, W. L.; Chandrasekhar, J.; Madura, J. D.; Impey, R. W.; Klein, M. L. *J. Chem. Phys.* **1983**, *79*, 926–935.
- (10) Essmann, U.; Perera, L.; Berkowitz, M. L.; Darden, T.; Lee, H.; Pedersen, L. G. *J. Chem. Phys.* **1995**, *103*, 8577–8592.
- (11) Yonetani, Y. *Chem. Phys. Lett.* **2005**, *406*, 49–53.
- (12) van der Spoel, D.; van Maaren, P. J. *J. Chem. Theory Comput.* **2006**, *1*, 1–11.
- (13) Berendsen, H. J. C.; van der Spoel, D.; van Drunen, R. *Comput. Phys. Commun.* **1995**, *91*, 43–56.
- (14) Lindahl, E.; Hess, B. A.; van der Spoel, D. *J. Mol. Model.* **2001**, *7*, 306–317.
- (15) van der Spoel, D.; Lindahl, E.; Hess, B.; Groenhof, G.; Mark, A. E.; Berendsen, H. J. C. *J. Comput. Chem.* **2005**, *26*, 1701–1718.
- (16) Mahoney, M. W.; Jorgensen, W. L. *J. Chem. Phys.* **2000**, *112*, 8910–8922.
- (17) Berendsen, H. J. C.; Postma, J. P. M.; van Gunsteren, W. F.; Hermans, J. In *Intermolecular Forces*; Pullman, B., Ed.; D. Reidel Publishing Company: Dordrecht, 1981; pp 331–342.
- (18) Berendsen, H. J. C.; Grigera, J. R.; Straatsma, T. P. *J. Phys. Chem.* **1987**, *91*, 6269–6271.
- (19) Starr, F. W.; Nielsen, J. K.; Stanley, H. E. *Phys. Rev. E* **2000**, *62*, 579–587.
- (20) Xu, H. F.; Stern, H. A.; Berne, B. J. *J. Phys. Chem. B* **2002**, *106*, 2054–2060.
- (21) Modig, K.; Pfrommer, B. G.; Halle, B. *Phys. Rev. Lett.* **2003**, *90*, 075502.
- (22) Modig, K.; Halle, B. *J. Am. Chem. Soc.* **2002**, *124*, 12031–12041.
- (23) Soper, A. K. *Chem. Phys.* **2000**, *258*, 121–137.
- (24) Luzar, A. *J. Chem. Phys.* **2000**, *113*, 10663–10675.
- (25) Luzar, A.; Chandler, D. *Nature* **1996**, *379*, 55–57.
- (26) Carey, D. M.; Korenowski, G. M. *J. Chem. Phys.* **1998**, *108*, 2669–2675.
- (27) Walrafen, G. E. *J. Chem. Phys.* **2004**, *120*, 4868–4876.
- (28) Edwards, H. G. M.; Farwell, D. W.; Jones, A. *Spectrochim. Acta, Part A* **1989**, *45*, 1165–1171.
- (29) Edwards, H. G. M.; Farwell, D. W. *J. Mol. Struct.* **1990**, *220*, 217–226.
- (30) Hiejima, Y.; Yao, M. *J. Chem. Phys.* **2003**, *119*, 7931–7942.
- (31) Sun, L.; Wick, C. D.; Siepmann, J. I.; Schure, M. R. *J. Phys. Chem. B* **2005**, *109*, 15118–15125.
- (32) Noskov, S. Y.; Lamoureux, G.; Roux, B. *J. Phys. Chem. B* **2005**, *109*, 6705–6713.

- (33) van Maaren, P. J.; van der Spoel, D. *J. Phys. Chem. B* **2001**, *105*, 2618–2626.
- (34) Lamoureux, G.; MacKerell, A. D.; Roux, B. *J. Phys. Chem. A* **2004**, *119*, 5185–5197.
- (35) Vorobyov, I. V.; Anisimov, V. M.; MacKerell, A. D., Jr. *J. Phys. Chem. B* **2005**, *109*, 18988–18999.
- (36) Hoffmann, M. M.; Conradi, M. S. *J. Phys. Chem. B* **1998**, *108*, 263–271.
- (37) Lalanne, P.; Andanson, J. M.; Soetens, J.-C.; Tassaing, T.; Danten, Y.; Besnard, M. *J. Phys. Chem. A* **2004**, *108*, 3902–3909.
- (38) Hess, B. *J. Chem. Phys.* **2002**, *116*, 209–217.
- (39) Hoffmann, M. M.; Conradi, M. S. *J. Phys. Chem. B* **1998**, *102*, 263–271.
- (40) Sciortino, F.; Fornili, S. L. *J. Chem. Phys.* **1989**, *90*, 2786–2792.
- (41) Ohmine, I.; Tanaka, H. *Chem. Rev.* **1993**, *93*, 2545–2566.
- (42) Luzar, A. *Faraday Discuss.* **1996**, *103*, 29–40.
- (43) Starr, F. W.; Nielsen, J. K.; Stanley, H. E. *Phys. Rev. Lett.* **1999**, *2294*–2297.
- (44) Agmon, N. *J. Phys. Chem.* **1996**, *100*, 1072–1080.
- (45) Schreiner, E.; Nicolini, C.; Ludolph, B.; Ravindra, R.; Otte, N.; Kohlmeyer, A.; Rousseau, R.; Winter, R.; Marx, D. *Phys. Rev. Lett.* **2004**, *92*, 148101.
- (46) van der Spoel, D.; van Maaren, P. J.; Berendsen, H. J. C. *J. Chem. Phys.* **1998**, *108*, 10220–10230.
- (47) Sheu, S. Y.; Yang, D. Y.; Selzle, H. L.; Schlag, E. W. *Proc. Natl. Acad. Sci. U.S.A.* **2003**, *100*, 12683–12687.
- (48) Efimov, A. V.; Brazhnikov, E. V. *FEBS Lett.* **2003**, *554*, 389–393.
- (49) Dill, K. A. *Biochemistry* **1990**, *29*, 7133–7155.
- (50) Pace, C. N. *Biochemistry* **2001**, *40*, 310–313.
- (51) Takano, K.; Scholtz, J. M.; Sacchettini, J. C.; Pace, C. N. *J. Biol. Chem.* **2003**, *278*, 31790–31795.
- (52) Privalov, P. L. In *Protein Folding*; Creighton, T. E., Ed.; Freeman: New York, 1992; pp 83–126.